Harmful Algae 127 (2023) 102471

Contents lists available at ScienceDirect

Harmful Algae

journal homepage: www.elsevier.com/locate/hal

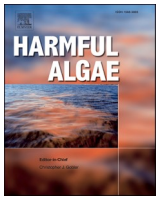

Production of the dinoflagellate *Amphidoma languida* in a large scale photobioreactor and structure elucidation of its main metabolite AZA-39

Rafael Salas [a,#,*], Elliot Murphy [a,b,#], Roisin Doohan [b], Urban Tillmann [c], Olivier P. Thomas [b]

[a] *Marine Institute, Rinville, Oranmore, H91 R673, Co. Galway, Ireland*
[b] *School of Biological and Chemical Sciences, Ryan Institute, University of Galway, University Road, H91TK33 Galway, Ireland*
[c] *Alfred Wegener Institut-Helmholtz Zentrum für Polar- und Meeresforschung Am Handelshafen 12, D-27570 Bremerhaven, Germany*

ARTICLE INFO

Edited By: Dr.Po Teen Lim

Keywords:
Azaspiracids
Amphidoma languida
AZA-39
Large scale cultivation
NMR
Dinoflagellate

ABSTRACT

Shellfish contamination with azaspiracids (AZA) is a major and recurrent problem for the Irish shellfish industry. *Amphidoma languida,* a small thecate dinoflagellate of the family Amphidomataceae, is widely distributed in Irish coastal waters and is one of the identified source species of azaspiracids. Irish and North Sea strains of *Am. languida* have been found to produce as major metabolites AZA-38 and -39 whose structures have only been provisionally elucidated by mass spectrometry and their toxic potential is currently unknown. In order to provide pure AZA-38 and -39 for subsequent structural and toxicological analyses, we present the first successful large-scale culture of *Am. languida*. A 180 L in house prototype bioreactor was used for culture growth and harvesting in semi-continuous mode for two months. Two different runs of the photobiorector with different light and pH setting showed the highest toxin yield at higher light intensity and slightly higher pH. AZA-38 and -39 cell quota were measured throughout the complete growth cycle with AZA-39 cell quota increasing in proportion to AZA-38 at late stationary to senescence phase. Over two experiments a total of 700 L of culture was harvested yielding 0.45 mg of pure AZA-39. The structure of AZA-39 was elucidated through NMR data analyses, which led to a revision of the structure proposed previously by mass spectrometry. While the spirotetrahydrofuran/tetrahydrofuran of rings A and B has been confirmed by NMR for AZA-39, a methyl is still present in position C-14 and the carboxylic acid chain is different from the structure proposed initially.

1. Introduction

Amphidomataceae is a growing family of Dinophyceae comprised of the small thecate genera *Azadinium* and *Amphidoma*, with few species known to produce azaspiracid toxins. Thus far, the genus *Azadinium* includes 16 species and most of them have been described in the last two decades (Salas et al., 2021; Tillmann et al., 2009). The genus *Amphidoma* currently comprises 12 species mainly described in the mid 20th century or before (Halldal, 1953; Kofoid and Michener, 1911; Schiller, 1929; Stein, 1883). Nevertheless, several species have been identified in the last decades such as *Amphidoma languida* Tillmann, Salas & Elbrächter (Tillmann et al., 2012), and other four *Amphidoma* species were added in 2018 after a long hiatus (Tillmann, 2018; Tillmann et al., 2018b). Species of Amphidomataceae have been thoroughly tested for the presence of toxic azaspiracids and most of them have been reported as non-producers. Azaspiracid production therefore appears to be more an exception than the rule for members of the Amphidomatacea family but other toxins might also be present (Salas et al., 2021). Among the genus *Azadinium*, two toxin producers inhabit the North Atlantic: *Azadinium spinosum* Elbrächter & Tillmann, 2009 (Krock et al., 2009; Tillmann et al., 2009), which is known to feature several ribotypes (Tillmann et al., 2021); and *Azadinium poporum* Tillmann & Elbrächter (Krock et al., 2012; Tillmann et al., 2011). Both species are known to produce a wide variety of toxic azaspiracid (AZA) metabolites. A third species, *Azadinium dexteroporum* Percopo & Zingone, 2013 (Percopo et al., 2013; Rossi et al., 2017) has been found to produce AZA, but so far only in the Mediterranean strains whereas other strains from the North Atlantic were found to be non-producers (Tillmann et al., 2015). For the genus *Amphidoma*, only one species *Am. languida* is known to produce AZA (Krock et al., 2012). The first strain of *Am. languida* was described in 2012 from a sample collected in the Southwest of Ireland, in Bantry bay (Tillmann et al., 2012), and since then, many other strains have been

* Corresponding author.
E-mail address: rafgall71@gmail.com (R. Salas).
# both authors contributed equally to this work.

https://doi.org/10.1016/j.hal.2023.102471
Received 8 February 2023; Received in revised form 27 May 2023; Accepted 10 June 2023
Available online 17 June 2023

isolated from different locations in the North Atlantic, including Iceland (Tillmann et al., 2015), Norway (Tillmann et al., 2018a), Greenland (Tillmann et al., 2020), and in the North Sea off the coast of Denmark and Scotland (Wietkamp et al., 2019). In 2017, a new strain was isolated in the Spanish Atlantic coast (Tillmann et al., 2017). Whereas this strain was found to produce AZA-2 and AZA-43, all other *Am. languida* strains from the North Sea and North Atlantic are known to produce AZA-38 and -39 as major metabolites.

Azaspiracids, first identified in *Az. spinosum* (e.g. AZA-1, -2), are known to cause symptoms in humans like DSP toxins, resulting in acute nausea, vomiting, diarrhea and stomach cramps. Initially, the isolation and purification of AZAs were achieved using naturally contaminated shellfish material (Satake et al., 1998). With the identification of *Az. spinosum* as the producer of AZA (Krock et al., 2009), large scale cultivation of Amphidomataceae opened an alternative source of toxins. In 2012, the cultivation of *Az. spinosum* in photobioreactors was the first successful attempt at isolating and purifying AZA-1 and -2 (Jauffrais et al., 2012). Since then, the other attempts at large scale culture have been the cultivation of two strains of *Az. poporum* for the isolation and purification of AZA-36 and -37 (Krock et al., 2015). The isolation of pure AZAs is of high relevance for both structure elucidation and toxicological bioassays, which are required to assess their potential toxicity. Moreover, the production of reference materials will ensure that analytical methods in marine biotoxin programs are improved and become effective tools for monitoring (Kilcoyne et al., 2019). The availability of large-scale cultures will also allow feeding studies in order to assess whether *Am. languida* is ingested by shellfish species and how the toxins are metabolized by the shellfish.

The main metabolites of *Am. languida* named AZA-38 and -39 have not yet been obtained in a pure form, and toxicity assays are consequently lacking on both compounds. To help mitigate any future intoxication events or unnecessary closures of shellfish farms, it is important to assess the relative toxicity of pure AZA-38 and -39 in AZA-1 equivalents. The main reason is that *Am. languida* has not been successfully cultivated at large scale, and highly contaminated shellfish samples, such as those of species of *Azadinium* used to extract and purify AZA-1 and -2, are not available. In this work, we describe the first successful attempt at growing *Am. languida* in a closed pH-controlled large scale photobioreactor in a semi-continuous system to produce the AZA congeners AZA-38 and -39. We report on the cell densities, toxin production and cell quota achieved during this study which culminated in the production of enough quantities of the pure major metabolite AZA-39 (0.45 mg) for structure elucidation. NMR analyses of this metabolite led to the revision of the structure proposed previously for AZA-39 based on MS data (Krock et al., 2012).

2. Materials and methods

2.1. Sample collection, isolation and culture of Amphidoma languida

The strain Z-LF-9-C9 of *Am. languida* was isolated in June 2016 during a survey on RV Uthörn from the southern North Sea off the Danish coast at 56°07′N, 07°28′E (Wietkamp et al., 2019). The strain was established after single cell isolation by microcapillary into wells of 96-well plates filled with 0.2 mL filtered seawater using a stereomicroscope (SZH-ILLD, Olympus) equipped with dark field illumination. The strain was routinely grown at 15 °C under a photon flux density of approx. 50 µmol m^{-2} s^{-1} on a 16:8 h light:dark photocycle. The strain was identified as *Amphidoma languida* by light microscopy (Fig. 1) and then confirmed by sequencing the D1/D2 region of the large subunit (LSU) of the ribosomal RNA genes (GenBank acc nr: MK613114). The strain was clonal but not axenic and was grown since its isolation in 2016 at the Alfred Wegener Institute in Germany in the standard conditions described above. In October 2019, the strain was transferred to the Marine Institute Ireland to start a large-scale culture reported here.

2.2. Photobioreactor

A closed photobioreactor (PBR) was built for this study. It was made from 15 mm thick transparent methacrylate sheets joined with a suitable silicone sealant for seawater aquarium and had the overall shape of an upside-down oversized tissue culture flask (Fig. 2). The PBR dimensions are 150 cm x 90 cm x 15 cm (Height: Width: Breadth) with an overall capacity of 180 L in volume (designed by Rafael Salas and built by Collins plastics, Ireland). The construction tapered at approximately 45° angle and 30 cm from the bottom.

At the bottom, a 5 cm bore hole was inserted to attach a tap with an open/close valve. The top of the construction had a lid perforated with 6 × 5 cm bore holes for air lines (x3), CO_2 line (x1), Vent (x1) and Oxygen and pH probes (x1). The methacrylate body including lid and bottom valve was held upright and at 30 cm from the ground by a stainless-steel frame with feet (Fig. 3).

The PBR was installed in a temperature-controlled room. This was fitted with 2 × 30 W, 1570 mm Length Linda LED strips (Filippi, Pianoro, Italy) around the perimeter of the incubator with incorporated on/off group switches to be able to modulate the amount of light in the incubator. The walk-in incubator is a temperature-controlled room fitted with a Dixel temperature control unit and a light timer switch system Flash Monotron 200 (Whiriskey, Claregalway, Ireland) to control the light and dark photoperiod. The walk-in incubator was also fitted with a CO_2 gas cylinder, pipe work and CO_2 manifolds for the delivery of this gas to the PBR.

2.3. Large scale cultivation of Amphidoma languida

2.3.1. Inoculation into the PBR

The seawater used in this experiment was collected at Ballyvaughan pier, Galway Bay (Lat: 53° 06′ 56′'N; Long: 9° 08′ 58′' W) using a SUB2020-SS submersible pump and a portable power generator Honda HX3000 (Honda, Minato, Tokyo, Japan) at high tide. The seawater was filtered using Whatmann ™ GF/F 0.44 µm nominal pore size using a Milli-vac vacuum pump placed in 1 L Teflon bottles and autoclaved at

Fig. 1. Live images of Amphidoma languida strain Z-LF-9-C9.

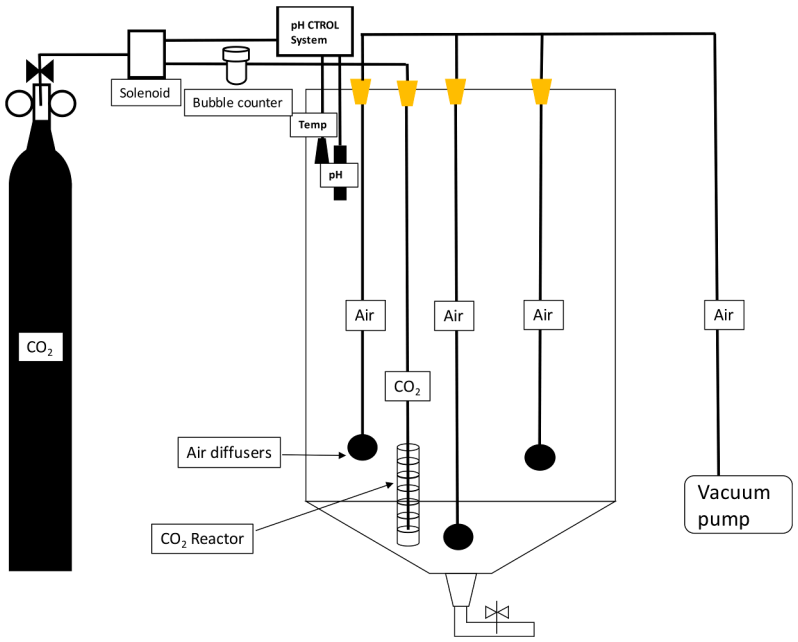

Fig. 2. Schematic of the in-house photobioreactor.

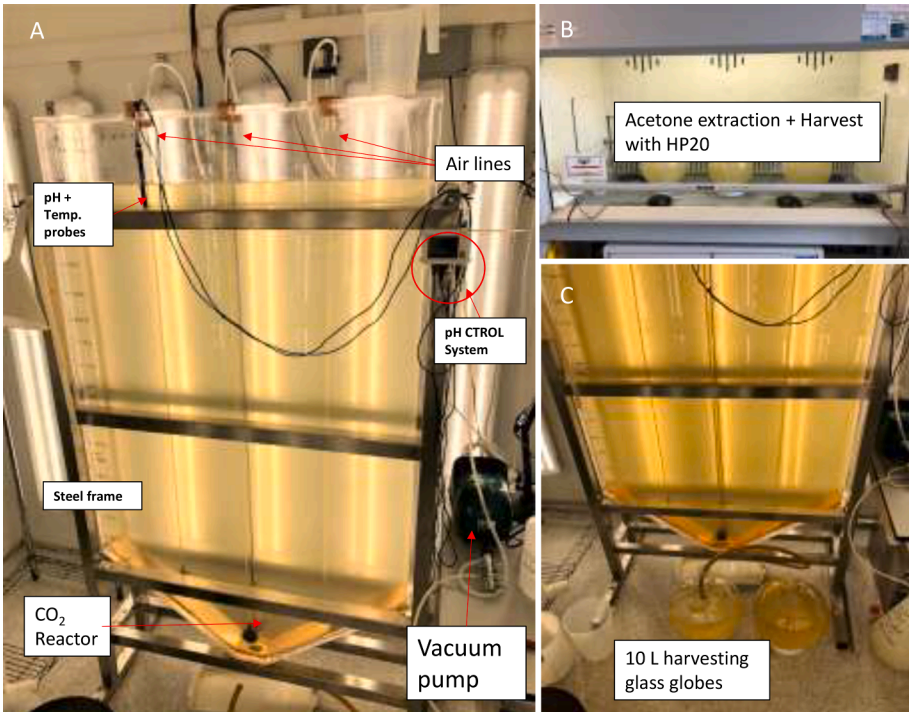

Fig. 3. (A) Photobioreactor system at full capacity. (B) HP20 extraction in a fumehood using 10 L round glass bottom flasks and (C) harvesting from PBR.

121 °C for 15 min. The water was placed in the walk-in incubator and equilibrated to the incubator temperature. Prior to inoculation, the PBR was cleaned with Decon 90® detergent for 24 h, followed by 10 full rinses with de-ionised water. Then the PBR was acid rinsed with a 1% Lancer rinse Acetic acid solution for 24 h. The PBR was rinsed again after the acid clean between 5 and 10 times with de-ionised water. After cleaning and disinfection, the PBR was primed with 30 L of sterile seawater to make sure that all the instrumentation worked for 24 h. This volume was disposed of before inoculation. After transfer from AWI Germany to MI Ireland, the culture was initially kept in an incubator at 15 °C and 12:12 L:D photoperiod in 1/10 strength K media and acclimatized to 18 °C and full-strength K media (Keller et al., 1987). The culture was scaled-up from 50 mL to 500 mL tissue culture flasks and from here to 5 L borosilicate Erlenmeyer flasks until it reached maximum cell density of approximately 30,000 to 80,000 cells mL^{-1}.

From these 5 L flasks, the PBR was initially inoculated at a maximum dilution rate of 3:1 inoculum: media to obtain minimum average cell densities in the photo-bioreactor of approximately 30,000 cells mL^{-1}. After this, the culture was scaled-up at intervals as the cell density increased by adding small increments of media into the photo-bioreactor of between 15 and 25% maximum dilution until it reached its maximum capacity of 180 L. The culture was grown in full strength K modified

media without ammonia and kept at 18 °C temperature and 12:12 L:D photoperiod. Aeration was delivered using a Blagdon Koi Air25 air pump (Blagdon Water Gardening, Dorking, Surrey) through 3 x air lines and submersed diffusers in the PBR at its lowest setting to avoid turbulence and shear stress of the culture. Aeration (to introduce gentle mixing) was only introduced in this experiment when the PBR was at full capacity and the culture was growing at a stable state in exponential phase.

The PBR set up was tested first with a strain of *Azadinium spinosum* and the pH maximum set point used was 8.3 +/- 0.1 hysteresis. A pH control system activates CO_2 addition into the system, by a solenoid valve, as the pH increases with cell growth above the maximum hysteresis value (8.4), the solenoid valve opens automatically to lower the pH to the lower hysteresis set point (8.2). When the pH probe measures below 8.2 the solenoid valve automatically shuts the flow of CO_2 into the system. The pressure at the manifold was set at approximately 4 psi which was the equivalent of 30–40 bubbles/minute using the bubble counter. This allowed for the steady but slow and controlled addition of CO_2 into the system, *via* the CO_2 reactor which was sitting just above the bottom of the PBR (Fig. 3).

2.3.2. Abiotic measurements

The following environmental parameters were measured daily during the large-scale experiment: The dissolved oxygen in the culture was measured using a DO meter Orion star A113 and the seawater pH was measured with an Orion 3 star (Thermo Fisher Scientific Waltham, Massachusetts, United States) pH benchtop pH meter. The pH control system JBL ProFlora® pH control Touch (JBL, Neuhofen, Germany), an off the shelf pH control system for Aquaria automatically monitored the pH in the PBR and kept it stable throughout the experiment at the chosen set point. This system included: (i) its own pH probe which was calibrated every 30 days and compared to the Orion benchtop meter; (ii) a temperature probe which was used to measure the seawater temperature against the air temperature read from the incubator Dixell temperature control system (Emerson, St. Louis, MO, United States); (iii) a CO_2 reactor submersed in the PBR and; (iv) a bubble counter and solenoid valve attached to the CO_2 in-house line system delivered by a CO_2 cylinder (BOC, Guilford, UK). The salinity was measured using an optical handheld refractometer Eclipse. Light intensity was measured using an ISO-Tech ILM350 digital light meter (RS components, Corby, UK) during culture growth over time.

2.3.3. Cell density measurements

PBR was first gently homogenized with a rigid plastic brush and increased aeration was used to continue the homogenization process for 1–2 min. After aeration was stopped, a volume of 3–5 L of culture was collected into a 5 L plastic container and the contents were poured back at the top of the photo-bioreactor. Then, a second volume of 3–5 L of culture was used to collect 3 × 1 mL samples pipetted out into 1.5 mL Eppendorf microtubes containing 20 μL of neutral lugol iodine.

From each sample, 1 mL was removed from the microtube and dispensed into a 1 mL glass Sedgewick-Rafter slide. The sample settled down for approximately 15 min before examination using an inverted microscope Olympus IX-51 (Olympus, Shinjuku City, Tokyo, Japan) or a Leica DMi8 (Leica Camera AG, Wetzlar, Germany) at x 400 magnification. At least 400 cells were counted in each sample from randomly chosen squares to obtain a minimum confidence limit of 90% (Andersen and Throndsen, 2004). Two successful runs in slightly different conditions are reported below.

2.3.4. PBR1 run

The pH in the system was set at 8.8 +/- 0.1 hysteresis. Mean temperature inside the PBR was stable at an average 19.9 °C during the study (Table S1). The light intensity inside the walk-in incubator was approximately 140 μmol m^{-2} s^{-1}, and the light intensity measured behind the photobioreactor (Table S1) corresponding to the light that has passed through the culture ranged between 70 and 91 μmol m^{-2} s^{-1}. The dissolved oxygen in the culture was above 100% saturation for the duration of the experiment but levels dropped from day 56 as the culture collapsed.

2.3.5. PBR2 run

Light intensity inside the walk-in incubator was reduced to approximately 70 μmol m^{-2} s^{-1}. pH set point for the addition of CO_2 in the system was slightly reduced from 8.8 to 8.75 +/- 0.1 hysteresis. The measurements of the different parameters during this second successful experiment are given in Table S4.

2.4. Toxin analysis

2.4.1. Analytical reagents and standards

All solvents (pestican-grade) were obtained from Labscan (Dublin, Ireland). Distilled water was purified further using a Barnstead nanopore diamond UV purification system (Thermo Fisher Scientific Waltham, Massachusetts, United States). Formic acid (≥98%), ammonium formate (>98%), Diaion HP20 polymeric resin (≥0.25 mm), and sodium periodate were from Sigma-Aldrich. CRMs for AZA-1 and -2 were obtained from the National Research Council (Halifax, NS, Canada).

2.4.2. Sample preparation for toxin analysis

During the first experiment (PBR1), samples for AZA analysis were collected in two ways. The PBR was first homogenised as in section 2.3.3, then;

(1) A simple and rapid extraction method called “vial extraction” used 100 μL sample aliquot placed into a glass HPLC vial equipped with an insert and 50 μL of methanol was pipetted into the vial to extract the sample. A volume of 2 μL of sample was injected into the LC-MS for AZA quantification.
(2) The second method used was based on Solid Phase Extraction (SPE). Samples were collected in 10 mL aliquots. The samples were stored in the -20 °C freezer until they were analysed. The 10 mL samples were defrosted at room temperature and then loaded onto a 1 g 6 mL Oasis Bond Elut cartridge, previously conditioned with MeOH 100% and H_2O 100%. The cartridge was then washed with H_2O (6 mL) followed by the elution of 15 mL of MeOH to recover azaspiracid toxins from the cartridge. The eluent was evaporated to dryness using miVac QUATTRO concentrator. The sample was then resuspended in 10 mL of MeOH and sonicated for 10 min. A volume of 1 mL was transferred *via* pipette and stored in 1.5 mL short thread vials for LC-MS analysis.

Both methods were compared only for the first experiment named PBR1 in 3.1 and the results are presented in the supplementary material. In the experiment PBR2 presented in 3.2, only the vial extraction method was used.

2.4.3. LC-MS analyses of AZA

This method was used to assess the concentration af AZAs along the purification steps of AZA-39 in 3.3. The harvested dried extracts were resuspended in 10 mL of MeOH under sonication for 10 min. A volume of 100 μL was transferred to 900 μL of MeOH and serially diluted 3 times. The third dilution was filtered using 1 mL syringe and 0.45 μm pore size syringe filters, transferred to a 1.5 mL LC-MS vial and stored at −20 °C until analysis.

Identification and quantification of toxins were performed on an Acquity UPLC coupled to a Xevo G2-S QToF (Waters, Manchester, UK). All analyses were performed in positive MSe (200–1200 *m/z*) and MS/MS modes. The reference compound used for calibration was leucine encephalin. The cone voltage was 40 V, collision energy was 50 V, the cone and desolvation gas flows were set at 100 and 1000 L h^{-1}, respectively, and the source temperature was 120 °C. Quantitation was

performed in MSe mode, using Targetlynx software. All toxins were quantitated against AZA-1. Mass transitions of 830>348 for AZA-38, 816>348 for AZA-39 and 842>672 for AZA-1 were used.

Binary gradient elution was used, with phase A consisting of water and phase B of 95% acetonitrile in water (both containing 2 mM ammonium formate and 50 mM formic acid). The column used was a 50 mm × 2.1 mm i.d., 1.7 μm, Acquity UPLC BEH C18 (Waters, Wexford, Ireland). The gradient was from 30 to 90% B over 6 min at 0.3 mL min^{-1}, held for 0.5 min, and returned to the initial conditions and held for 1 min to equilibrate the system. The injection volume was 2 μL and the column and sample temperatures were 25 °C and 6 °C, respectively.

2.5. Toxin extraction, purification and structure elucidation in the bulk cultures

2.5.1. Culture harvest

A semi-continuous harvesting strategy was used for *Am. languida*. This involved harvesting regularly a defined volume of culture and replenishing the photo-bioreactor with K media. Approximately 30 L of culture were harvested from the PBR into 3 × 10 L borosilicate round bottomed flasks. Cells in the flasks were lysed by addition of acetone to final concentration of 7% (Kilcoyne et al., 2019). Previously activated HP20 resin was then added (2 g L^{-1}). The mixture was agitated under constant aeration for 48 h to keep the resin in suspension. Using a 80 μm nytex mesh, the resin was separated from the supernatant and stored wet at 4.0 °C in water. This procedure was repeated for a total of 700 L of culture over two experiments (PBR1 = 250 L; PBR2 = 450 L).

2.5.2. Extraction

To determine the quantity of AZA-38 and -39 recovered per harvest during the first run PBR1, the HP20 resin (60 g) was first dried overnight in the fume hood. The resin was then suspended in MeOH (200 mL) and stirred for 2 h. Methanol was then separated using a glass chromatography column (8 cm diameter, 60 cm length). Further portions of MeOH (150 mL) were eluted through the column dropwise. A volume of 100 μL of each elution were added to 900 μL of MeOH and their AZA content was quantified using the LC-MS. Elution continued until the concentration of AZA-39 was <1.0 ng mL^{-1} in the column eluent. Eluent was combined and dried in a rotary evaporator under reduced pressure. The dried extract was stored at -20 °C.

Toxin extraction during the second run PBR2 was conducted as above with slight variations. Instead of drying the HP20 resin from each harvest separately, the HP20 resin from several harvests was combined to three portions of 450 g and dried. The amount of methanol used for the extraction was 800 mL with further portions of 600 mL and the chromatography column was 15 cm in diameter.

2.5.3. Purification

The extracts were initially purified using the SPE method. Our separation conditions followed the conditions used in Krock et al. (2015). The sample was suspended in 20% CH_3CN (16 mL). The sample was then split into portions (2 mL) and loaded onto a previously conditioned C_{18} SPE cartridge (500 mg 6 mL). Four fractions of decreasing polarity were recovered: (A) H_2O:MeOH (9:1 v/v, 15 mL), (B) H_2O:MeOH (4:6 v/v), (C) H_2O:MeOH (2:8 v/v, 30 mL) and (D) MeOH (100%, 30 mL). Fractions were tested for AZA content and fractions C and D were combined (442 mg, all weights recorded in this part are of dried residues) as they both contained the compounds of interest and dried under reduced pressure. The resulting fraction was then suspended in MeOH (10 mL) and sonicated (10 min). The sample was stored at -20 °C for 30 min. Then, the supernatant was collected *via* pipette, and this was repeated 2 times to separate the AZAs from any insoluble material. The resulting dried fraction (292 mg) was dissolved in 3.5 mL of MeOH and fractionated further using preparative HPLC with a C_{18} column (Waters, X-Select CSH, 19 × 250 mm, 5 μm) under isocratic conditions (27:73 H_2O:CH_3CN + 2.0 mM ammonium acetate). Peaks 5–7 (3.55 mg) contained AZA-38 and were combined and peaks 2–4 (2.88 mg) contained AZA-39 and were combined separately. Final purification of AZA-39 was performed using a C_{18} column (Waters, SymmetryPrep, 7.5 × 300 mm, 5 μm) under isocratic conditions (1:1 H_2O:CH_3CN + 2.0 mM ammonium acetate). AZA-39 was finally desalted using a method published in Krock et al. (2015) to lead 0.45 mg of pure material. Unfortunately, the purification of AZA-38 from peaks 5–7 did not afford enough pure material for NMR analyses.

NMR analyses on AZA-39 were performed in CD_3OD at 25 °C with the residual peak of CD_3OD (δ_H 3.31 ppm δ_C 49.0 ppm) used as references on a Varian 600 MHz equipped with a cryoprobe. A mixing of 0.3 s was used for the 1D TOCSY experiment while 0.5 s was used for the ROESY experiment.

3. Results

3.1. PBR1: first Am. languida large-scale culture

3.1.1. Cell densities and toxin monitoring

The initial inoculum had an average cell density estimate of approximately 28,000 cells mL^{-1} but as the cell density was decreasing during the first days, *Am. languida* inoculum and K-media were added in days 4 and 14 (Fig. 4, gray bars) to 105 L capacity. In days 22, 24 and 28 the K-NH_4 medium was added to bring the PBR to full capacity (Fig. 4, Red bars) and K-NH_4 nutrient stock solution for 180 L was subsequently added in days 32 and 49 (Fig. 4, triangles).

In day 28, the PBR was at full capacity (180 L) (Fig. 4, arrow) and the culture commenced its exponential phase, with the highest cell density of 75,000 cells mL^{-1} achieved in day 34.

The growth rate was calculated at the exponential phase, from day 28 (PBR at full capacity) to day 34 (first harvest). The growth rate (μ) for this seven-day period was 0.122 d^{-1} (corresponding to a doubling time of 5.7 days). The decision was made to harvest 30 L of the culture at day 34 and then harvest regularly the same volume every 2–3 days based on culture cell density recovery. Biomass was then harvested in days 34, 37, 41, 45, 49 and, as the culture commenced its senescence phase, two more harvests took place in days 56 and 57 (Table 1). From day 49 onwards, the PBR was not replenished with new media after harvest as the culture was not recovering. No more measurements were recorded after day 57, although two more harvests took place thereafter. The pH measured for the duration of the PBR1 (Fig. 4, grey rhombs) ranged between 8.5 to 8.85 and then decrease with lower cell densities after day 49.

The cell quota calculated from the SPE extractions plotted against the cell density estimate was consistent throughout the experiment and did not differ greatly, except when the culture had entered its senescence phase (Fig. 5). Here, cell numbers declined drastically and the relation between total toxins and cell density was not meaningful and thus omitted. Both methods described in 2.4.2 were used and compared in this first experiment to assess the toxin content of the cells. We decided to select the vial method over the SPE method as the obtained results were less variable (See Figure S1). The ratio of AZA-38 to -39 ranged between 0.51 and 0.98 (Table 1) with most data points falling between 0.6 and 0.8 AZA-38 to -39. The ratio of toxins appeared to be independent of the cell concentration but decreased as the culture collapsed (days 53 to 57) to minimum AZA-38 to -39 ratios of about 0.5 (Table S3).

3.1.2. PBR1 harvests using HP20

From 250 L harvest of cells in PBR1, quantification of AZA-38 and -39 in the extract by LC-MS estimated 301 μg of AZA-38 and 394 μg of AZA-39 using AZA-1 as reference (Table 2). There was a slight increase in toxin concentration extracted from harvests 5 to 9 (average: 1.9 μg L^{-1}) compared to harvests 1 to 4 (average: 1.5 μg L^{-1}). In these concentrated biomass extract, the phosphorylated versions of both AZA-38 and -39 were also detected.

There was an increase in toxin cell quota during harvest 5 (31.7 fg

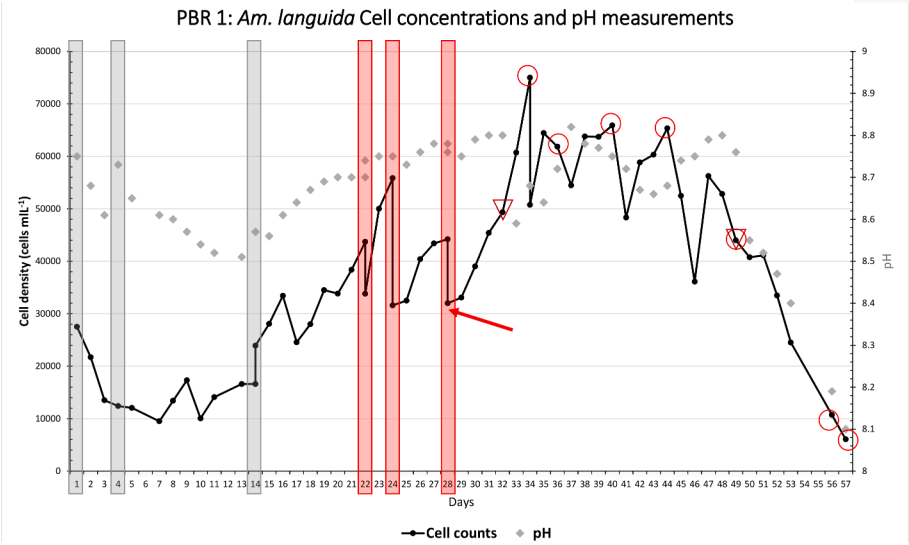

Fig. 4. Amphidoma languida cell densities and pH measurements during PBR1. Grey bars indicate inoculation days; Red bars indicate media addition with cell measurements before and after. Arrow indicates PBR at full capacity. Triangles indicate when K-NH_4 nutrient stock was added, and red circles indicate harvests.

Table 1
PBR1 harvests, cell densities and HP20 AZA results.

Harvests	Vol. harvested (L)	Cell density Cells mL^{-1}	AZA-38 fg $cell^{-1}$	AZA-39 fg $cell^{-1}$	AZA-38 µg	AZA-39 µg	AZA-38/39 Ratio
1	30	75,000	10.7	11.8	24.2	26.6	0.91
2	30	61,833	16.0	18.0	39.6	33.5	0.88
3	30	65,905	18.1	19.8	35.8	39.2	0.91
4	20	65,333	18.2	20.4	23.8	26.7	0.89
5	30	44,000	31.7	40.1	41.9	52.9	0.79
6	30	10,700	117	166	37.5	53.6	0.70
7	30	6058	238	333	43.3	60.6	0.71
8	30	*	*	*	43.2	63.8	*
9	20	*	*	*	21.5	36.8	*
Total	250	*	*	*	301	394	*

* No cell density measurements taken from harvest 7 onwards as culture crashed.

$cell^{-1}$ AZA-38 and 40.1 fg $cell^{-1}$ AZA-39) as the culture started its decline. This was comparable with our SPE results for the same day (19.6 fg $cell^{-1}$ AZA-38 and 32.4 fg $cell^{-1}$ AZA-39), indicating the start of the senescence phase.

3.2. PBR2 2nd Am. languida large scale run

The water temperature was on average 19.4 °C during the second run and the dissolved oxygen measurements were on average 20% higher than in the previous run PBR1, suggesting some level of oxygen over-saturation. pH measurements during the second run were more variable compared to PBR1 (Tables S1 and S4), with low pH values recorded for example in days 29 (8.30), 47 (8.33), 54 (8.37) and 57 (8.37). This phenomenon may be partially explained by the addition of new media

Table 2
Summarized toxin data for PBR1 and PBR2 vial method comparison.

PBR2 toxin data	Vials AZA-38 (ng mL^{-1})	Vials AZA-38 (fg $cell^{-1}$)	Vials Aza-39 (ng mL^{-1})	Vials AZA-39 (fg $cell^{-1}$)	Ratio AZA-38 to AZA-39
Average	1.94	19.18	2.20	21.77	0.88
median	1.39	16.28	1.69	19.06	0.82
Minimum	0.56	5.55	0.96	8.27	0.59
Maximum	5.79	48.78	6.15	51.75	0.94

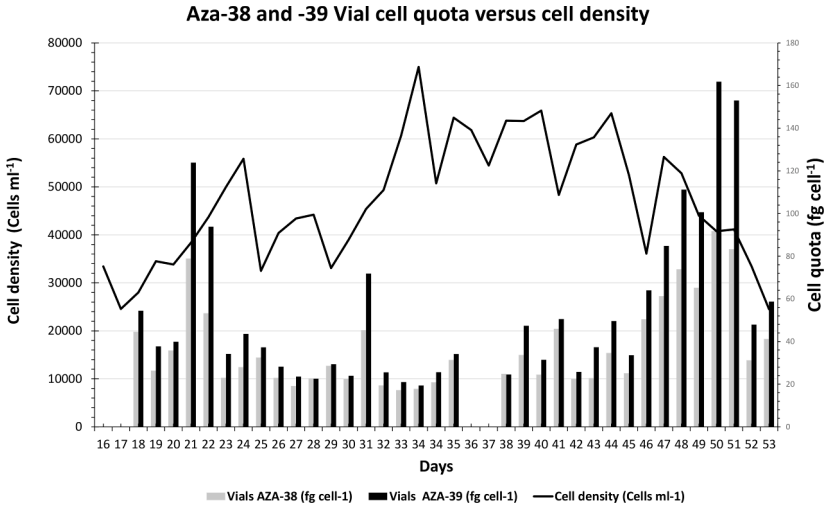

Fig. 5. AZA-38 and 39 Vial cell quota and cell densities in PBR1.

after harvests and by the addition of CO_2 into the system that have the net effect of lowering the pH.

3.2.1. Cell densities and toxin monitoring

For PBR2, the PBR was initiated with 50 L inoculum at an average cell density estimate of 7000 cells mL^{-1}. During the first 10 days, there was no evidence of growth, so in day 11 an extra 10 L of culture was inoculated to increase the cell density to approximately 15,000 cells mL^{-1} (Fig. 6). Medium was added on days 14 (40 L), 18 (35 L) and 21 (45 L) to bring the PBR to full capacity. The cell density at full capacity was 45,100 cells mL^{-1} and the highest cell density estimate was recorded in day 46 (131,400 cells mL^{-1}). Nutrients were added with K-NH_4 nutrient stock for 180 L in days 28, 43 and 54. The growth rate for PBR2 was calculated for a seven day period (day 25 to day 32). The growth rate (μ) for PBR2 was 0.099 d^{-1}.

PBR2 was harvested on eight days (red circles in Fig. 6) The first six harvests were performed during late exponential and stationary phase, while the two last harvests on days 54 and 57 were collected during senescent phase when cell densities declined. After each harvest, the PBR was brought back to full capacity and the 180 L were harvested and extracted.

On average, the toxin amounts for PBR2 were 1.94 ng mL^{-1} AZA-38 and 2.20 ng mL^{-1} AZA-39 (Table 2). However, the cell quota was half in PBR2 compared to PBR1, as similar amount of toxins was found in twice the cell density for PBR2. The average ratio of AZA-38 to 39 toxins was similar in both experiments, but higher AZA-38 amounts were found compared to AZA-39 in PBR2 (0.88) than in PBR1 (0.76).

Cell quotas for PBR2 up to day 48 (except day 19) were generally low with quotas ranging from 10 to 20 fg $cell^{-1}$ (Fig. 7). From days 49 to 55, there was a large increase in cell quota when the culture entered late stationary to senescence phase. The ratio of AZA-38 to -39 measured in PBR2 was consistent across the experiment with most measurements around 0.8, except for day 19 with a higher ratio (1.4) and days 25, 29 and 48 which were slightly lower between 0.6 and 0.7.

3.2.2. PBR2 harvests using HP20

For PBR2, the HP20 resin from successive harvests were pooled into two large batch extractions. The first 6 harvests for a total of 200 L were in batch 1 and the next two harvests (100 L) and the remaining 180 L from the photobioreactor made batch 2 to a total of 250 L.

During this process, 454 μg of AZA-38 and 567 μg of AZA-39 were estimated by LC-MS in the extracts. The ratio of AZA-38/39 was higher for batch 1 (exponential phase) compared to batch 2 (late exponential-senescence phase). In total, between the two experiments, both lasting approximately 2 months each, 755 μg of AZA-38 and 961 μg AZA-39 in the raw extracts were estimated by LC-MS. The next step was therefore the purification of these two toxins which resulted in enough toxin for structure elucidation only for AZA-39. The purification of AZA-38 was also attempted but the purity of the resulted AZA-38 was not sufficient to confirm the previous proposed structure.

3.3. Purification and structure elucidation of AZA-39

AZA-39 was purified from the HP20 extracts of both PBR1 and PBR2 combined adapting procedures previously described. Four isolation steps were required to purify AZA-39 from the HP20 extracts. A total weight of 450 μg of AZA-39 was recovered from 700 L of *Am. languida* cultures (Table 3).

AZA-39 was obtained as an off white crystalline solid with a protonated molecule $[M + H]^+$ at *m/z* 816.4893 corresponding to the molecular formula $C_{45}H_{69}NO_{12}$. The identity of AZA-39 was confirmed by its MS/MS spectrum being identical to the one published originally, and characterized by the absence of the group 5 fragment formed from the retro-Diels-Alder cleavage at *m/z* 672 and the presence of fragments 1–4 at *m/z* 448.3055 ($C_{26}H_{42}NO_5^+$), 348.2532 ($C_{21}H_{34}NO_3^+$), 248.1645 ($C_{15}H_{22}NO_2^+$) and 154.1227 ($C_9H_{16}NO^+$) (Krock et al., 2012). This unusual fragmentation pattern suggested structural changes were expected close to the carboxylic acid or ring A of the molecule compared to the reference compound AZA-1. The structure of AZA-37 was previously reported using NMR in CD_3OD, and therefore the structure elucidation of AZA-39 was undertaken by comparison with the NMR data of this compound (Table 4) (Krock et al., 2015). The ^1H NMR spectrum of AZA-39 exhibited one less oxymethine signal at δ_H 4.39 and one extra methyl at δ_H 1.05 (d, J = 6.5 Hz, CH_3–8) when compared to the NMR data of AZA-37 (Fig. 8, Table 2).

The key H-4/H-5/H-6/H-7/H-8/H-9a and b and H-8/H-Me-8 COSY correlations established the new spin coupled system and the location of the additional methyl signal as Me-8 (Fig. 9). The key H-Me-8/C-8/C-7/C-9 HMBC correlations confirmed the location of the additional methyl at C-8. The configuration of the additional olefin was assigned as *E* based on the value of the coupling constant $^3J_{5,6}$ of 10 Hz. A probable partial structure shown in Fig. 9a was first proposed based on analogies with AZA-1 and the likely presence of the additional olefin in the ring A. Even if no HMBC correlation was clearly observed with the carboxylic acid,

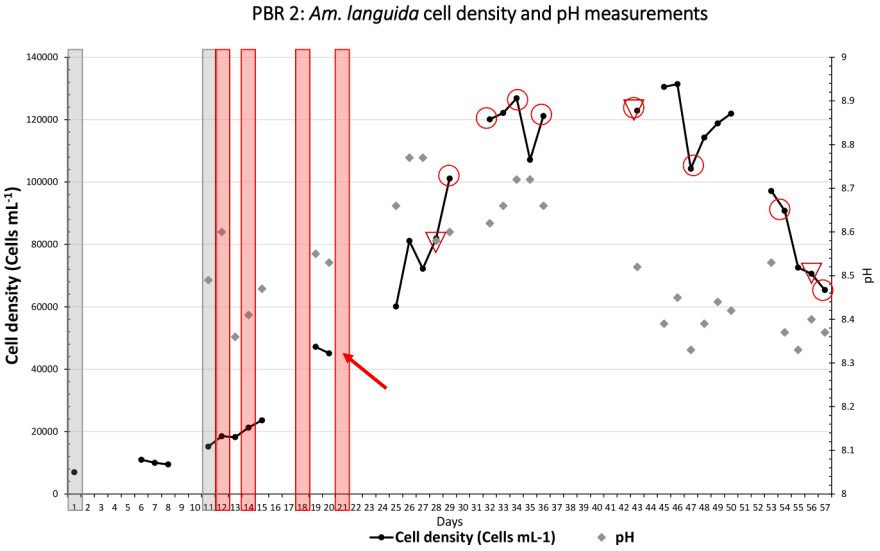

Fig. 6. Amphidoma languida PBR2 growth curve and pH measurements. gray bars indicate inoculation days; red bars indicate media addition Arrow indicates PBR at full capacity. Triangles indicate nutrients addition, red circles indicate harvests.

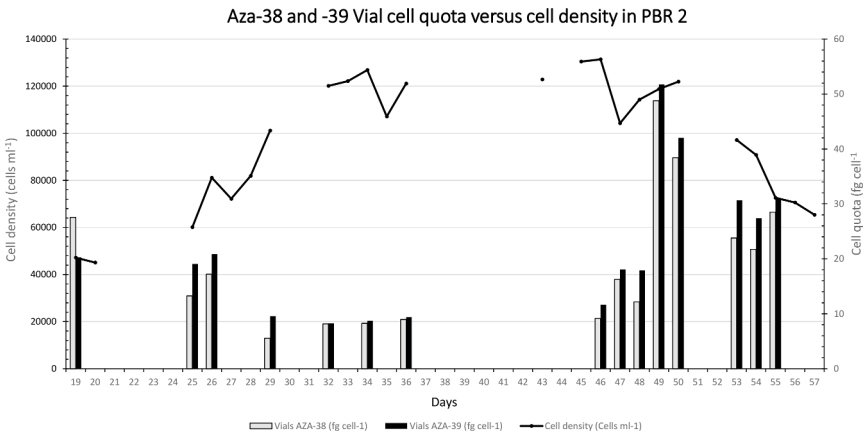

Fig. 7. AZA-38 and 39 Vials cell quota and cell densities in PBR2.

Table 3
Summary table for purification of AZA-39.

Step No	Step	AZA-39 [µg]	Weight [g]	Purity [%]*
	HP20 resin extract	960	2.92	0.03
1	SPE	760	0.44	0.17
2	Salt precipition	650	0.29	0.22
3	Prep HPLC (C_{18})	290	<0.01	10
4	Semi-prep HPLC (C_{18})	450	–	95
	% Recovery (steps 1–4)	47		

* Based on w/w and quantification by MS using AZA-1 as standard.

HMBC correlations with the new spirocarbon at δ_C 116.4 (C-10) disproved this hypothesis. Indeed, the key H-Me-8/H-9/H-11/H-12/C-10 HMBC correlations placed the methylene at C-9 connected to the carbon C-10 and not the carboxylic acid (Fig. 9b). The chemical shift of the spiroat C-10 is more deshielded than expected for AZAs and hints at more strain in the ring systems providing further evidence of a 5-membered ring instead of a 6-membered ring for other AZAs. Additionally, a 1D TOCSY showed that signals from H-4 to H-8 and also H-Me-8 were present in the same spin coupled system further highlighting the presence of the 5-membered ring. The remaining moiety of the molecule was consistent with AZA-37 and was confirmed by 1D and 2D-NMR experiments. The configuration at C-20 for all AZAs is consistent with the last conclusions drawn following the total synthesis of AZA-3 and the reassignment of this configuration (Kenton et al., 2018a, 2018b) The numbering for AZA-39 as shown in Fig. 8 was preferred to be consistent with other AZA reported, highlighting a plausible biosynthetic consistency corresponding to one acetate unit less for AZA-39 compared to AZA-1.

As AZA-39 is the first azaspiracid with a 5-membered ring A, we then investigated the configurations of the three chiral centers at C-7, C-8 and C-10, considering that the other configurations were conserved with AZA-1. First, the key H-Me-8/H-7 and H-8/H-6 nOes were consistent with a *trans* relative configurations with the substituents at C-7 and C-8 (Fig. 9c). Among the four remaining possibilities, a key H-6/H-Me-14 NOE allowed us to propose the most likely relative configurations between all substituents as depicted in Fig. 9. This NOE can only be observed if the oxygen of the ring A is placed on the opposite side of the oxygen of ring C and if the olefin at C-5/C-6 is oriented upwards in the same direction as Me-14. Finally, as epimerisation was observed at C-37 when AZA-1 was purified in acidic medium we wanted to ensure the configuration at C-37 for the purified AZA-39 (Kilcoyne et al., 2014a). The reported comparison of NMR data for AZA-2 and its 37-*epi* derivative was extremely useful to conclude that the isolated AZA-39 is not an epimer at C-37. For example, H-20 resonates at δ_H 3.85 in AZA-39 which is very similar to $\delta_{H\text{-}20}$ 3.82 for AZA-2 and distinct to $\delta_{H\text{-}20}$ 3.50 for 37-*epi*-AZA-2. Similar conclusions could be drawn through comparisons

Table 4
^{1}H- (600 MHz) and ^{13}C NMR (150 MHz) chemical shifts for AZA-37 (Krock et al., 2015) and AZA-39 in CD_3OD.

Position	AZA-37			AZA-39		
	δ_C	δ_H mult. (*J* in Hz)		δ_C	δ_H mult. (*J* in Hz)	
1	180.3	–	–	–	–	–
2	46.1	2.33	–	–	–	–
3	71.4	4.39	–	179.8	–	–
4	134.6	5.70	–	37.6	2.99 dd (16, 7)	3.03 dd (16, 7)
5	133.1	5.65	–	129.2	5.85 dt (10, 7)	–
6	73.3	4.35	–	132.3	5.44 t (10)	–
7	38.4	1.43	1.87	83.1	4.30 t (9)	–
8	22.2	1.70	1.77	40.6	2.18 m	–
9	36.6	1.70	1.83	46.6	1.77 m	2.20 m
10	109.1	–	–	116.4	–	–
11	33.9	1.69	2.33	34.8	1.92 m	2.25 m
12	32.8	1.83	2.03	33.8	1.66 m	2.22 m
13	111.8	–	–	110.0	–	–
14	31.8	2.01	–	30.8	1.98 m	–
15	33.5	1.76	1.87	32.5	1.76 m	1.83
16	78.9	3.94	–	78.0	3.91 br s	–
17	74.3	4.29	–	73.4	4.26 br s	–
18	37.6	2.00	2.07	37.0	2.01 m	2.07 m
19	79.9	4.44	–	79.1	4.43 dt (8, 6)	–
20	77.4	3.93	–	76.8	3.85 br s	–
21	101.0	–	–	100.1	–	–
22	37.6	2.07	–	36.5	2.11 m	–
23	39.1	1.43	1.43	38.2	1.43 m	–
24	43.0	1.35	–	42.2	1.36 m	–
25	80.3	4.00	–	79.6	3.98 d (9.5)	–
26	149.0	–	–	148.1	–	–
27	50.4	2.25	2.42	49.3	2.23 d (14)	2.40 d (14)
28	99.4	–	–	98.5	–	–
29	45.0	1.36	2.05	44.2	1.35 m	2.02 m
30	27.2	2.23	–	26.3	2.24 m	–
31	36.1	1.52	1.84	35.3	1.52 td (13.5, 4)	1.84 dd (14, 4)
32	73.7	4.37	–	72.8	4.35 d (3.5)	–
33	82.1	4.05	–	80.7	3.99 br s	–
34	75.7	5.00	–	75.0	4.96 m	–
35	42.7	2.49	2.60	42.1	2.38 m	2.56 dd (14, 4)
36	98.0	–	–	97.7	–	–
37	36.7	1.98	–	36.4	1.91 m	–
38	29.7	1.63	–	29.4	1.67 m	1.66 m
39	23.8	1.70	–	23.5	1.77 m	1.65 m
40	41.2	2.99	3.17	40.4	2.89 br d (12.5)	3.13 dd (14, 12.5)
8-Me				15.8	1.037 (d, 6.5)	–
14-Me	17.5	0.90	–	16.0	0.916 d (6.5)	
22-Me	17.2	0.92	–	16.3	0.905 (d, 6.5)	
24-Me	18.9	0.84	–	18.0	0.825 (d, 6.5)	
26-CH_2	117.8	5.15	5.33	116.7	5.14 br s	5.31 br s
30-Me	24.3	0.96	–	23.5	0.945 d (6.5)	–
37-Me	16.4	0.97	–	15.6	0.945 d (6.5)	–

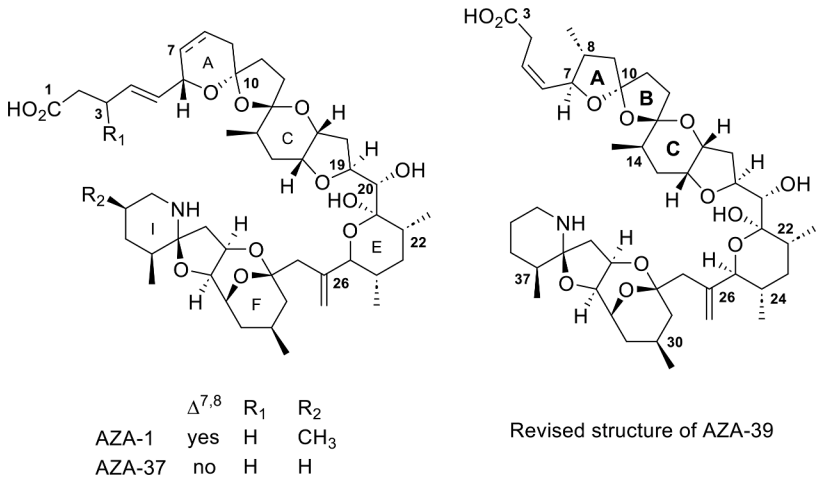

	$\Delta^{7,8}$	R_1	R_2
AZA-1	yes	H	CH_3
AZA-37	no	H	H

Fig. 8. Structures of the known AZA-1 (Kenton et al., 2018a) and -37 (Krock et al., 2015) together with the revised structure of AZA-39 (Krock et al., 2012).

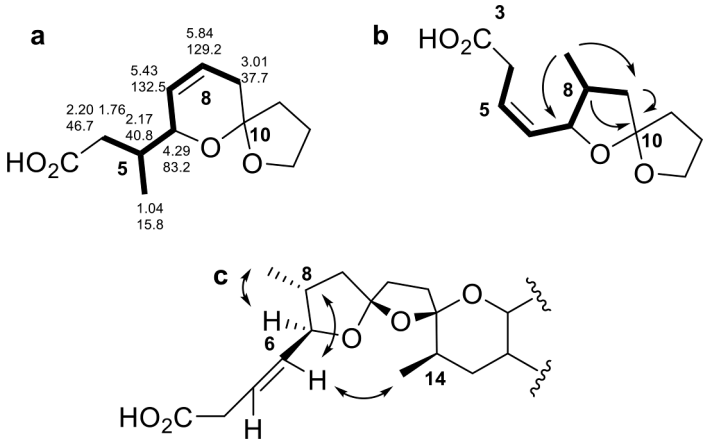

Fig. 9. a. Partial structure first postulated for AZA-39 using NMR data. b. key COSY and HMBC correlations for the correct partial structure of AZA-39. c. key nOes for the relative configurations of the partial structure of AZA-39.

of all other signals. We are therefore confident to conclude on the full 3D structure of AZA-39.

4. Discussion

Some strains of *Am. languida* have been established successfully as laboratory cultures over the last couple of years (Wietkamp et al., 2020, 2019). However, this species is more difficult to maintain and grow in laboratory conditions on the long run, when compared to other small Amphidomataceae species. For example: *Az. spinosum* and *Az. poporum* have been kept in culture conditions for years and have been grown successfully in large scale for toxin production without major difficulties (Jauffrais et al., 2012; Krock et al., 2015). In contrast, the type strain SM1 of *Am. languida* was lost a few years after its isolation from two different laboratories and from both culture collections where the strains had been deposited. In addition, growth of *Am. languida* in the laboratory is generally quite slow, cell densities remain low, and strains seem to be sensitive to stress as they hardly survive shipping from one laboratory to another (own unpublished results). Potential reasons for such a general sensitivity of *Am. languida* are unknown, but with the present work of a first successful mass culture of an *Am. languida* strain, few parameters are identified which seem to be crucial in this successful attempt. Microscopic observation of the newly inoculated cultures in the PBR showed that *Am. languida* sensitively reacted to this change, as live cells readily shed their thecal plates (a process called ecdysis). While ecdysal cells can remain viable and recover, cell densities in both PBR setups initially declined indicating that a significant number of cells died. This problem was overcome by using repeated inoculations (e.g. three times in the first two weeks in PBR1) to counteract stress-induced cell loss and to allow the PBR culture to eventually start exponential growth. The preliminary attempts at establishing *Am. languida* in large scale failed and it is most likely due to the sensitivity of this species to stress. Additionally, altering the pH set point (i.e. the pH when CO_2 addition starts) from 8.30 (used in the two preliminary attempts) to substantially higher values (> 8.7) enabled to successfully establish the culture in large scale for the first time. For PBR2 the system was adjusted by reducing the pH set point from 8.80 to 8.75 and halving the light intensity. With a set point of 8.80 in fact no CO_2 was added at all because pH value above 8.91, the threshold point for CO_2 to be added into the system, was not reached. Observing the development of the culture in the PBR2 conditions, it became clear that while the growth rates between PBR1 and PBR2 were similar (μ= 0.122 and 0.099 respectively), *Am. languida* benefitted in terms of maximum cell densities achieved from the changed conditions. The similar growth rate indicates that growth was not light limited when light intensity was halved in PBR2, but a potential role of reduced light for the increase in maximum cell densities is not clear. In contrast, the potential effect of adding more CO_2 to the system on an increase in final cell yield is plausible. The cell density improved almost two-fold from PBR1 (max cell density = 75,000 cells mL^{-1}) to PBR2 (max. cell density = 131,400 cells mL^{-1}). However, higher cell densities were not coupled to higher toxin yield as the toxin cell quota were lower in PBR2 compared to PBR1. Taking into

consideration the differences of final cell yield and toxin yield between PBR1 and PBR2, a combination of factors increasing cell yield combined with factors favoring toxin yield will likely improve and optimize this system further. Both successful runs lasted 60 days each approximately and from them a total of 700 L of biomass with an equivalent raw toxin content of 755 μg and 961 μg of AZA-38 and -39, respectively, was harvested. Both runs of the PBR indicate that CO_2 limitation and light intensity play an important role, but additional replicated experiments including controls, and also considering effects of nutrient limitation (P, N) should be performed to better define an optimal combination of environmental factors for an optimized cell and toxin yield of *Am. languida* in large-scale cultures.

The AZA cell quota varied in the two runs. The vial method used here covers both intra- and extracellular toxins, and direct comparisons with literature reports on cell quotas obtained from cell pellets is difficult. Generally, high variability in cell quota among strains of *Am. languida* (Tillmann et al., 2021), and also intra-strain variability, partly depending on the growth phase of the culture, have already been reported (Wietkamp et al., 2019). Here, AZA ratio changed overtime during the culture life cycle, while AZA-38 amounts were maintained. The difference in the AZA-38/-39 ratio between exponential phase compared to late stationary to senescence phase (Tables 1, 2) suggests that an increase in AZA-39 compared to AZA-38 occurs at the onset of senescence phase. A first laboratory study reported for strain Z-LF-9-C9 high AZA-38 amounts and an AZA-38/-39 ratio of 1.18, which was substantially higher than the range of 0.38 to 0.69 reported for all other most *Am. languida* strains (Wietkamp et al., 2019), and also substantially higher than the toxin ratio reported here for the same strain (between 0.6 and 0.8). This high variability of the AZA-38/-39 ratio shows that it is not a constant trait for the species or for a specific strain.

For harvesting, a semi-continuous system was chosen in which a replacement of the harvested volume with new culture medium allowed a stable system to run and to produce cells and toxins for a longer time. In total, between the two studies we extracted 700 litres of culture corresponding to 755 μg of AZA-38 and 961 μg of AZA-39 assessed by MS, which are not dissimilar to the amounts accomplished during the *Az. poporum* study where similar comparable volumes were worked on (Krock et al., 2015).

In an attempt to improve yield of toxin, different purification steps were used. An initial C_{18} SPE step was employed instead of a liquid-liquid partition or silica gel step normally used for purification of AZAs. This step returned a decent yield of 76% and a reduction of 85% which was comparable to recoveries seen for silica gel and liquid-liquid partitions (Kilcoyne et al., 2014b). We had initially tested the SPE method on extracts containing AZA-1 and had high recoveries of 90–103% for AZA-1 (data not shown). The recovery of AZA-39 using SPE was slightly lower at 79%. The sample per SPE cartridge might have been too high in salt concentration for the 500 mg cartridges, saturating them and may have reduced the recovery for AZA-39. When attempting to resolubilize the sample in MeOH, insoluble material was present as salts which remained partly after the SPE. The salts were finally removed through precipitation in portions of MeOH with a recovery of 86%. Following this, two consecutive HPLC steps resulted in the purification of AZA-39. Recovery from the preparative HPLC was unexpectedly low, as it is normally reported with recoveries of >90%. Finally, the recovery of 450 μg of AZA-39 suggested that the ionization potential was different compared to AZA-1 and that the amount of AZA-39 has been underestimated in the previous quantifications vs AZA-1. Unfortunately, although both initial quantities of AZA-38 and -39 were relatively close, the amount of purified AZA-38 recovered was not of sufficient purity to conclude on its structure. ^{1}H NMR spectrum of the peaks containing AZA-38 provide some information on the olefinic signals but with the high degree of signal overlap in other regions of the spectrum it is impossible to conclude where the loss of the hydroxyl group is located when comparing to the shifts reported for AZA-37.

The structure for AZA-39 was originally postulated in 2012 through MS/MS fragmentation analysis (Krock et al., 2012). It contained a tetrahydrofuran ring for A as a response to the absence of the typical fragment at *m/z* 672 in the CID spectra of AZA-39. A pseudo Retro-Diels-Alder (RDA) reaction is known to be responsible for the fragmentation of the dihydropyrane ring A. Here, the presence of the tetrahydrofuran ring was confirmed through NMR data but the locations of some methylenes have been corrected. Importantly an additional methyl was undoubtedly located at C-8. The ^{13}C NMR chemical shift of the first spirocenter at δ_C 116.4 was more deshielded than expected for AZAs (δ 108–110) hinting at a change in electron density around this position and attributed to the ring contraction from 6 to 5 members. The fragmentation pattern of AZA-39 differs from AZA-38 and suggests that the easy cleavage of the terminal carboxylic acid may be induced by the presence of the double bond at C-5 leading to a stabilised allylic carbocation. Importantly, the purified compound will be used to commence *in vitro* and *in vivo* studies. As AZA-39 is the first azaspiracid with a 5 membered ring A, toxicity assays on this compound will bring essential data for future monitoring of these toxins in the North Atlantic.

5. Conclusion

The first successful bulk culturing of the species *Am. languida* is presented using a prototype photobioreactor. The reactor was designed in-house and purpose built for the continuous production of sensitive planktonic microalgal biomass. From the HP20 extracts harvested from the *Am. languida* cultures, we were able to purify 450 μg of the major metabolite AZA-39. Using 1D and 2D NMR experiments, the structure of AZA-39 was revised from the first proposition obtained by LC-MS/MS. This study shows how structures postulated from MS fragmentation data are important but should be reassessed whenever possible with NMR experiments. Following this successful isolation of AZA-39, its toxicity relative to AZA-1 is currently under study and will be reported elsewhere.

Declaration of Competing Interest

The authors declare that they have no known competing financial interests or personal relationships that could have appeared to influence the work reported in this paper.

Data availability

Data will be made available on request.

CRediT authorship contribution statement

Conceptualization, R.S.; PBR design and construction, R.S.; Methodology, R.S. and E.M.; Large scale culture, R.S. and E.M.; Cell measurements, R.S. and E.M.; strain isolation, characterization and original culture, U.T.; Chemical analysis, E.M. and R.D; Large scale harvest, E.M. and R.S.; Investigation, R.S., E.M., O.T; Original draft preparation, R.S.; Review and editing, R.S., E.M., U.T., and O.T. Project administration, O. T. All authors have read and agreed to the published version of the manuscript.

Acknowledgments

EM received a PhD scholarship from the Marine Institute under the Marine Research Programme by the Irish Government [grant number CF/18/03/01, Cullen fellowship]. The authors wish to thank Dave Clarke and Jane Kilcoyne on technical support and helping with acquiring pieces of equipment and materials used during this study. We would like to thank Bernd Krock for his contribution and discussions on the structure of AZA-39. Also, we wish to thank Mox Henderson whose help liaising with Collins plastics in the building of the photobioreactor

and steel frame was essential and Joe Silke for some fruitful discussions.

Supplementary materials

Detailed experimental procedures for PBR1 and PBR2 are reported together with NMR data for AZA-39 and AZA-38.

Supplementary material associated with this article can be found, in the online version, at doi:10.1016/j.hal.2023.102471.

References

Andersen, P., Throndsen, J., 2004. Estimating cell numbers. In: Hallegraeff, G.M., Anderson, D.M., Cembella, A.D. (Eds.), Manual On Harmful Marine Microalgae. UNESCO, Paris, France, pp. 99–129.

Halldal, P., 1953. Phytoplankton investigations from weather ship M in the Norwegian Sea, 1948-49. (Including observations during the "Armauer Hansen" cruise, July 1949.). Norske VidenskAkad. Hvalråd. Skr 38, 1–91.

Jauffrais, T., Kilcoyne, J., Séchet, V., Herrenknecht, C., Truquet, P., Hervé, F., Bérard, J. B., Nulty, C., Taylor, S., Tillmann, U., Miles, C.O., Hess, P., 2012. Production and Isolation of Azaspiracid-1 and -2 from Azadinium spinosum Culture in Pilot Scale Photobioreactors. Mar. Drugs 1360–1382.

Keller, M.D., Selvin, R.C., Claus, W., Guillard, R.R.L., 1987. Media for the Culture of oceanic ultraphytoplankton. J. Phycol. 23 (4), 633–638.

Kenton, N.T., Adu-Ampratwum, D., Okumu, A.A., McCarron, P., Kilcoyne, J., Rise, F., Wilkins, A.L., Miles, C.O., Forsyth, C.J., 2018a. Stereochemical Definition of the natural product (6R,10R,13R, 14R,16R,17R,19S,20S,21R,24S,25S,28S,30S,32R,33R,34R,36S,37S,39R)-Azaspiracid-3 by total synthesis and comparative analyses. Angew. Chem. Int. Edit. 57 (3), 810–813.

Kenton, N.T., Adu-Ampratwum, D., Okumu, A.A., Zhang, Z., Chen, Y., Nguyen, S., Xu, J., Ding, Y., McCarron, P., Kilcoyne, J., Rise, F., Wilkins, A.L., Miles, C.O., Forsyth, C.J., 2018b. Total synthesis of (6R,10R,13R,14R,16R,17R,19S,20R,21R,24S, 25S,28S,30S,32R,33R,34R,36S,37S,39R)-Azaspiracid-3 reveals non-identity with the natural product. Angew. Chem. Int. Edit. 57 (3), 805–809.

Kilcoyne, J., McCarron, P., Twiner, M.J., Nulty, C., Crain, S., Quilliam, M.A., Rise, F., Wilkins, A.L., Miles, C.O., 2014a. Epimers of Azaspiracids: isolation, Structural Elucidation, Relative LC-MS response, and in vitro toxicity of 37-epi-Azaspiracid-1. Chem. Res. Toxicol. 27 (4), 587–600.

Kilcoyne, J., McCoy, A., Burrell, S., Krock, B., Tillmann, U., 2019. Effects of temperature, growth media, and photoperiod on growth and toxin production of Azadinium spinosum. Mar. Drugs 17 (9), 489.

Kilcoyne, J., Nulty, C., Jauffrais, T., McCarron, P., Herve, F., Foley, B., Rise, F., Crain, S., Wilkins, A.L., Twiner, M.J., Hess, P., Miles, C.O., 2014b. Isolation, structure elucidation, relative LC-MS response, and in vitro toxicity of Azaspiracids from the Dinoflagellate Azadinium spinosum. J. Nat. Prod. 77 (11), 2465–2474.

Kofoid, C.A., Michener, J.R., 1911. New genera and species of dinoflagellates. Bull. Mus. Comp. Zool. Harvard College 54 (22), 267–302.

Krock, B., Tillmann, U., John, U., Cembella, A.D., 2009. Characterization of azaspiracids in plankton size-fractions and isolation of an azaspiracid-producing dinoflagellate from the North Sea. Harmful Algae 8 (2), 254–263.

Krock, B., Tillmann, U., Potvin, É., Jeong, H.J., Drebing, W., Kilcoyne, J., Al-Jorani, A., Twiner, M.J., Göthel, Q., Köck, M., 2015. Structure elucidation and in vitro toxicity of new azaspiracids isolated from the marine dinoflagellate Azadinium poporum. Mar. Drugs 6687–6702.

Krock, B., Tillmann, U., Voß, D., Koch, B.P., Salas, R., Witt, M., Potvin, É., Jeong, H.J., 2012. New azaspiracids in Amphidomataceae (Dinophyceae). Toxicon 60 (5), 830–839.

Percopo, I., Siano, R., Rossi, R., Soprano, V., Sarno, D., Zingone, A., 2013. A new potentially toxic Azadinium species (Dinophyceae) from the Mediterranean Sea, A. dexteroporum sp. nov. J. Phycol. 49 (5), 950–966.

Rossi, R., Dell'Aversano, C., Krock, B., Ciminiello, P., Percopo, I., Tillmann, U., Soprano, V., Zingone, A., 2017. Mediterranean Azadinium dexteroporum (Dinophyceae) produces six novel azaspiracids and azaspiracid-35: a structural study by a multi-platform mass spectrometry approach. Anal. Bioanal. Chem. 409 (4), 1121–1134.

Salas, R., Tillmann, U., Gu, H., Wietkamp, S., Krock, B., Clarke, D., 2021. Morphological and molecular characterization of multiple new Azadinium strains revealed a high diversity of non-toxigenic species of Amphidomataceae (Dinophyceae) including two new Azadinium species in Irish waters. North East Atlantic. Phycol. Res. 69 (2), 88–115.

Satake, M., Ofuji, K., Naoki, H., James, K.J., Furey, A., McMahon, T., Silke, J., Yasumoto, T., 1998. Azaspiracid, a new marine toxin having unique spiro ring assemblies, isolated from Irish mussels, Mytilus edulis. J. Am. Chem. Soc. 120 (38), 9967–9968.

Schiller, J., 1929. Über eine biologische und hydrographische Untersuchung des Oberflächenwassers im westlichen Mittelmeer im August 1928. Bot. Arch. 27, 381–419.

Stein, F., 1883. Die Naturgeschichte der Arthrodelen Flagellaten. Einleitung und Erklärung der Abbildungen. Wilhelm Engelman, Leipzig, Germany.

Tillmann, U., 2018. Electron microscopy of a 1991 spring plankton sample from the Argentinean Shelf reveals the presence of four new species of the Amphidomataceae (Dinophyceae). Phycol. Res. 66 (4), 269–290.

Tillmann, U., Edvardsen, B., Krock, B., Smith, K.F., Paterson, R.F., Voß, D., 2018a. Diversity, distribution, and azaspiracids of Amphidomataceae (Dinophyceae) along the Norwegian coast. Harmful Algae 80, 15–34.

Tillmann, U., Elbrächter, M., John, U., Krock, B., 2011. A new non-toxic species in the dinoflagellate genus Azadinium: A. poporum sp. nov. Eur. J. Phycol. 46 (1), 74–87.

Tillmann, U., Elbrächter, M., Krock, B., John, U., Cembella, A., 2009. Azadinium spinosum gen. et sp. nov. (Dinophyceae) identified as a primary producer of azaspiracid toxins. Eur. J. Phycol. 44 (1), 63–79.

Tillmann, U., Gottschling, M., Guinder, V., Krock, B., 2018b. Amphidoma parvula (Amphidomataceae), a new planktonic dinophyte from the Argentine Sea. Eur. J. Phycol. 53 (1), 14–28.

Tillmann, U., Gottschling, M., Nézan, E., Krock, B., 2015. First records of Amphidoma languida and Azadinium dexteroporum (Amphidomataceae, Dinophyceae) from the Irminger Sea off Iceland. Mar. Biodivers. Rec. 8, e142.

Tillmann, U., Jaén, D., Fernández, L., Gottschling, M., Witt, M., Blanco, J., Krock, B., 2017. Amphidoma languida (Amphidomatacea, Dinophyceae) with a novel azaspiracid toxin profile identified as the cause of molluscan contamination at the Atlantic coast of southern Spain. Harmful Algae 62, 113–126.

Tillmann, U., Salas, R., Gottschling, M., Krock, B., O'Driscoll, D., Elbrächter, M., 2012. Amphidoma languida sp. nov. (Dinophyceae) Reveals a Close Relationship between Amphidoma and Azadinium. Protist 163 (5), 701–719.

Tillmann, U., Wietkamp, S., Gu, H., Krock, B., Salas, R., Clarke, D., 2021. Multiple new strains of amphidomataceae (Dinophyceae) from the North Atlantic revealed a high toxin profile variability of Azadinium spinosum and a New Non-Toxigenic Az. cf. spinosum. Microorganisms 9 (1), 134.

Tillmann, U., Wietkamp, S., Krock, B., Tillmann, A., Voss, D., Gu, H., 2020. Amphidomataceae (Dinophyceae) in the western Greenland area, including description of Azadinium perforatum sp. nov. Phycologia 59 (1), 63–88.

Wietkamp, S., Krock, B., Clarke, D., Voß, D., Salas, R., Kilcoyne, J., Tillmann, U., 2020. Distribution and abundance of azaspiracid-producing dinophyte species and their toxins in North Atlantic and North Sea waters in summer 2018. PLoS ONE 15 (6), e0235015.

Wietkamp, S., Krock, B., Gu, H., Voß, D., Klemm, K., Tillmann, U., 2019. Occurrence and distribution of Amphidomataceae (Dinophyceae) in Danish coastal waters of the North Sea, the Limfjord and the Kattegat/Belt area. Harmful Algae 88, 101637.